Advances in Science and Technology Research Journal

Advances in Science and Technology Research Journal, 2026, 20(2), 529–551
https://doi.org/10.12913/22998624/213623
ISSN 2299-8624, License CC-BY 4.0

Received: 2025.09.22
Accepted: 2025.12.15
Published: 2025.12.23

Investigation of the fresh and hardened properties of fly ash and metakaolin based geopolymer concrete containing of nanoparticles

Ayad Saddam Alwan[1], Mojtaba Fathi[1*]

[1] Department of Civil Engineering, Faculty Engineering, Razi University, Kermanshah, Iran
* Corresponding author's email: aliowaid13@gmail.com

ABSTRACT

The global construction sector faces significant sustainability challenges due to the high energy consumption and carbon emissions associated with ordinary Portland cement (OPC). Geopolymer concrete (GPC), synthesized through the alkali activation of aluminosilicate-rich by-products such as fly ash (FA) and metakaolin (MK), offers a promising low-carbon alternative. This study examines the effects of combining FA, MK, nano-alumina (NA), and nano-limestone (NL) in binary, ternary, and quaternary GPC blends of GP-40 and GP-60. Hardened properties, including compressive, flexural, and splitting tensile strengths, along with ultrasonic pulse velocity, were evaluated at 7, 28, 56, and 90 days. The results showed that nanomaterials improved pore structure and binder homogeneity, leading to enhanced overall mechanical performance. Optimized mixes achieved compressive strengths exceeding 55 MPa at 90 days, with significant improvements in splitting tensile and flexural strengths. The results indicate that nanomodified GPC blends demonstrated balanced performance, making them a sustainable alternative for future green concrete applications.

Keywords: geopolymer concrete; fly ash; metakaolin; nano-alumina, nano-limestone, fresh and mechanical properties.

INTRODUCTION

Concrete is the most widely used construction material worldwide, ranking second only to water in terms of consumption. Its widespread use is attributed to its high mechanical properties, durability, and adaptability to various environmental conditions. However, ordinary Portland cement (OPC), the primary constituent of conventional concrete, has been widely criticized for its substantial environmental impact. Cement manufacturing contributes approximately 8% of global anthropogenic CO_2 emissions equivalent to about 0.8–1.0 tons of CO_2 per ton of cement produced [1–5], and requires extensive consumption of natural resources and thermal energy. These environmental challenges have motivated ongoing research efforts to develop more sustainable and eco-efficient alternatives capable of reducing the carbon footprint without compromising mechanical performance or structural reliability [6, 7]. In this context, geopolymer concrete has emerged as one of the most promising low-carbon alternatives [8, 9]. Geopolymers are inorganic binders synthesized through the alkaline activation of aluminosilicate precursors, representing a distinct class of materials fundamentally different from OPC, which hardens through the hydration of calcium silicate phases [10, 11]. This distinct reaction mechanism can reduce CO_2 emissions by up to 80% compared with OPC [12], and provides superior resistance to aggressive environments, elevated temperatures, and chemical degradation [13, 14]. Among the aluminosilicate precursors used in geopolymer synthesis, fly ash (FA) and metakaolin (MK) have gained significant

research attention due to their wide availability and favorable pozzolanic reactivity.

Fly ash, a byproduct of coal combustion in thermal power plants, consists of fine, spherical particles rich in silica and alumina that exhibit high pozzolanic activity. According to ASTM C618, FA is classified into Class F (low-calcium) and Class C (high-calcium) types [15–17]. Class F provides superior pozzolanic behavior, while Class C shows partial self-cementing ability. With an estimated annual global production of 600–900 million tons, fly ash represents both an environmental burden and a valuable resource for sustainable concrete technologies [18].

Numerous studies have shown that substituting 20–40% of OPC with FA enhances long-term strength, improves durability through reduced permeability, and lowers CO_2 emissions by 20–30% [19–21]. In geopolymer systems, FA reacts with alkaline activators – typically sodium hydroxide and sodium silicate – to form sodium aluminosilicate hydrate (N–A–S–H) gels, which densify the microstructure and contribute to strength development [22]. However, its relatively low reactivity under ambient curing conditions often limits early-age strength [23], prompting researchers to adopt thermal curing or nanomaterial incorporation to accelerate geopolymerization [24].

MK, on the other hand, is a highly reactive aluminosilicate derived from calcined kaolin clay at 600–800 °C, producing an amorphous pozzolanic material with consistent chemical purity [25]. Unlike FA, MK is purposefully manufactured, ensuring uniformity and high reactivity. Partial replacement of OPC with 5–20% MK has been reported to enhance both compressive and tensile strength, improve durability, and reduce porosity [26–28]. These improvements are primarily attributed to the refinement of pore structure and the formation of additional binding phases, such as C–S–H and hydrated aluminosilicates, in alkaline environments [29, 30]. MK-based geopolymers can achieve compressive strengths exceeding 50 MPa within 28 days under ambient curing, demonstrating high resistance to chloride ingress, sulfate attack, and thermal degradation [31, 32].

While FA is abundant and cost-effective, its slow reaction kinetics limit its standalone performance. In contrast, MK exhibits faster geopolymerization and higher early strength but at the expense of workability and cost. Consequently, current research emphasizes binary and ternary FA/MK systems to achieve an optimized balance between cost, workability, reactivity, and mechanical performance [33, 34]. Recent studies have further highlighted that incorporating nanomaterials such as nano-silica, nano-alumina, and nano-lime into FA/MK-based geopolymers refines the pore structure, accelerates polycondensation reactions, and significantly improves overall performance and microstructural uniformity [35–39].

Despite significant progress in geopolymer research, several challenges remain, particularly in achieving adequate early-age strength under ambient curing conditions, minimizing shrinkage, and ensuring long-term durability in chemically aggressive environments. Recent global studies emphasize the urgent need for a systematic evaluation of binary and ternary FA-MK geopolymer systems modified with nanomaterials, aimed at achieving an integrated balance between mechanical performance and environmental sustainability.

In response to these challenges, the present study aims to develop and evaluate different grades of geopolymer concrete (GP-40 and GP-60, which are experimental codes and not standard concrete grades), produced using fly ash and metakaolin as primary precursors, and incorporating nano-alumina (NA) and nano-limestone (NL) as modifying agents to enhance performance. The mixtures are activated with an alkaline solution and cured under ambient temperature conditions to simulate practical field applications. The study investigates the fresh properties of the developed geopolymer concretes, including workability (slump) and bulk density, along with their mechanical properties, such as compressive strength, split tensile strength, and flexural strength. Additionally, non-destructive evaluation is conducted using ultrasonic pulse velocity (UPV) to assess internal homogeneity and structural integrity.

EXPERIMENTAL PROGRAM

Materials

In this study, a combination of pozzolanic and nano-materials, along with conventional constituents of concrete, was employed to develop geopolymer concrete with enhanced mechanical performance and durability. These materials include FA, MK, NA, NL, in addition to the alkaline activator

solution (AAS), fine and coarse aggregates, water, and a superplasticizer admixture. A detailed description of these materials is provided below.

Aluminosilicate materials (FA and MK)

Low-calcium fly ash (Class F, ASTM [13]) and metakaolin were employed as the primary aluminosilicate sources in this study. The fly ash was obtained from local thermal power plants, whereas metakaolin was produced through the calcination of pure kaolin at 600–800 °C. This endothermic process involves the removal of chemically bonded hydroxyl groups, which disrupts the crystalline lattice of kaolin. This disruption generates a reactive amorphous phase rich in silica and alumina, thereby imparting high pozzolanic activity. Chemical and physical tests for both materials were conducted at the National Center for Construction Laboratories and Research (NCCLR) in Babylon. The results, summarized in Table 1, show that fly ash contains high percentages of SiO_2 and Al_2O_3, providing suitable pozzolanic activity, while metakaolin is one of the purest and most reactive pozzolanic materials with a high specific surface area that enhances geopolymerization reactions.

Nanoparticles (NA (Al_2O_3) and NL ($Ca(OH)_2$))

Nanoparticles were incorporated in this study as highly pure materials to enhance the reactivity of geopolymer concrete. Nano alumina (NA), with 99.99% purity and an average particle size of 60–80 nm, primarily consists of spherical-phase crystals. These crystals provide exceptional reactivity with binder materials, accelerating geopolymerization reactions. The specific surface area ranges from 15 to 40 m²/g. Similarly, nano limestone (NL), composed of calcium hydroxide nanoparticles with an average size of 20–80 nm and a purity of ≥94.5%, exhibits a specific surface area of 30–80 m²/gm and rapid solubility in water, thereby promoting pozzolanic reactions when combined with silica and alumina rich sources such as fly ash and metakaolin. The properties of NA and NL particles, as reported by the manufacturer, are summarized in Table 2.

Table 2. Properties of NL and NA

Property	Test results *	
	NL	NA
Physical form	Powder	Powder
Color	White	White
Particle size, nm	20–80	60–80
Specific gravity	3.2	2.4
purity %	95-99	99.99
Crystal	alpha	spherical
Specific surface area (m²/gm)	30–80	15–40
Fe %	≤0.005	-
Si %	≤0.003	-
Mg %	≤0.001	-
Ca $(OH)_2$ %	-	≥ 94.5

Note: *The test results from the manufacturer

Table 1. Chemical compositions and physical properties of fly ash and metakaolin

Property	Materials	FA	MK
Chemical composition (%)	(SiO_2)	51.0	51.7
	(Al_2O_3)	29.9	35.4
	(Fe_2O_3)	10.6	2.72
	(CaO)	2.24	1.38
	(MgO)	0.77	0.82
	(Na_2O)	0.01	0.73
	(K_2O)	2.02	0.84
	(SO_3)	0.26	0.24
	(P_2O_5)	1.65	0.43
	(TiO_2)	1.71	0.92
	(LOI)	0.46	3.42
Physical properties	Physical form	Powder	Powder
	Colour	Light grey	Off-White
	Median particle size (μm)	12.8	14.3
	Specific surface area (m²/kg)	463	1640
	Specific gravity	2.60	2.62

Alkaline activator solution (AAS)

The alkaline activator solution is a fundamental component in geopolymer production due to its ability to dissolve silica and alumina and to catalyze polymerization reactions [40]. In this study, commercial sodium hydroxide flakes with 99% purity were dissolved in distilled water to prepare a 12 M solution (362 g/L) following [41, 42], and the solution was left for 24 hours before being mixed with sodium silicate solution. The activator was prepared with a mass ratio of 2.0 between Na_2SiO_3 and NaOH, while maintaining an activator-to-binder ratio of 0.52 for grade GP40 and 0.47 for grade GP60, which enhances the reactivity with the source materials [43]. The properties of the sodium silicate used, as provided by the manufacturer, are presented in Table 3.

Aggregates

In this study, Natural sand from Al-Ukhaider and crushed washed gravel from Al-Nabai'i were used as fine and coarse aggregates, respectively. The physical properties of the fine aggregate included a specific gravity of 2.65, water absorption of 2.63%, fineness modulus of 2.46, sulfate content of 0.38%, and 1.94% passing the 0.075 mm sieve. The coarse aggregate exhibited a specific gravity of 2.6, water absorption of 0.6%, and sulfate content of 0.07%. All tests were conducted according to ASTM standards [44] at the Construction Materials Laboratory, University of Babylon.

Table 3. Properties of sodium silicate utilized in this study

Description	Value
Na_2O % by weight	13.0–13.4
SiO_2% by weight	31–33
Viscosity (CPS) 20 °C	650-1250
Specific Gravity	1.538–1.557
Density - 20 °C	53 ± 0.5
Appearance	Hazy
Ratio of SiO_2 / Na_2O	2.3± 0.05

Super plasticizer (SP)

The high-performance polycarboxylate-based superplasticizer, commercially known as Sika Visco Crete 180G, was used to reduce water demand and improve the workability of geopolymer concrete (GPC). This superplasticizer, produced by Sika (Type F), complies with ASTM standards [45], and its optimal dosage should be determined through site trials to ensure the desired concrete performance.

Mix proportions of geopolymer concrete

The detailed mix proportions of the geopolymer concrete (GPC) used in this study are presented in Tables 4 and 5. The mix design methodology was developed empirically based on the performance of trial mixes and material characteristics, in accordance with general principles of ACI guidelines, but not derived directly from any specific standard procedure. Table 4 summarizes the binary mixes for GP40 and GP60 grades, where fly ash (FA) was partially replaced

Table 4. The mixing proportions of Binary mixes

Mix. No	Mix grade	L/B	Quantities of ingredients (kg/m³)							
			Binder	FA (%)	MK (%)	NaOH	Na_2SiO_3	F. A	C. A	SP %
M1	GP-40	0.52	415	100	0	72	144	748	1030	1.2
M2	GP-40	0.52	415	90	10	72	144	748	1030	1.2
M3	GP-40	0.52	415	80	20	72	144	748	1030	1.2
M4	GP-40	0.52	415	70	30	72	144	748	1030	1.2
M5	GP-40	0.52	415	60	40	72	144	748	1030	1.2
M6	GP-40	0.52	415	50	50	72	144	748	1030	1.2
M7	GP-60	0.47	520	100	0	81	162	720	947	1.5
M8	GP-60	0.47	520	90	10	81	162	720	947	1.5
M9	GP-60	0.47	520	80	20	81	162	720	947	1.5
M10	GP-60	0.47	520	70	30	81	162	720	947	1.5
M11	GP-60	0.47	520	60	40	81	162	720	947	1.5
M12	GP-60	0.47	520	50	50	81	162	720	947	1.5

by metakaolin (MK) at varying percentages (0%, 10%, 20%, 30%, 40%, and 50%). The binder content, alkaline activator solution (NaOH and Na_2SiO_3) at a ratio of 2, and the ratios of fine aggregate, coarse aggregate, and binder are provided for each grade. For GP40 mixes, these ratios are 1:1.8:2.5 with a superplasticizer dosage of 1.2% and a liquid-to-binder (L/B) ratio of 0.52, whereas for GP60 mixes, the ratios are 1:1.4:1.82 with a superplasticizer dosage of 1.5% and an L/B ratio of 0.47. These ratios were chosen to balance workability and mechanical strength, ensuring proper hydration, required flowability for mixing, and adequate strength and durability in the hardened state. The detailed compositions of the ternary and quaternary geopolymer concrete mixes are presented in Table 5. Nano-alumina (NA) and nano-calcite (NL) were added to the optimized blend of 70% fly ash and 30% metakaolin at replacement levels of 2%, 3%, and 4% by mass. The ratios of binder, fly ash, metakaolin, NA, NL, alkaline activator solution, aggregates, and superplasticizer for each mix remain similar to those of the binary mixes, allowing a systematic evaluation of the effects of nano-materials on the performance of GP40 and GP60 concrete.

Mixing, casting, curing, and testing procedures of geopolymer concrete

The primary distinction between geopolymer concrete (GPC) and conventional concrete lies in the type of binder used, where silica and alumina present in FA and MK react with the alkaline solution (Na_2SiO_3 and NaOH) to form a geopolymer paste that binds the coarse and fine aggregates along with other ingredients to produce the concrete. The mixing method plays a critical role in influencing the workability and strength of GPC. All mixing procedures were conducted in a laboratory at 25±2 °C using a pan-type laboratory mixer with a capacity of approximately 0.09 m³, ensuring that the mixer was kept clean, wet, and free of residual materials before each batch. The alkaline solution was prepared in advance, left for 20 minutes, and then used as the liquid component after adding water and superplasticizer. The mixing steps began with combining the dry materials (coarse and fine aggregates, FA, and MK) for 2.5 minutes, after which the prepared liquid containing the alkaline solution, water, and superplasticizer was gradually added over 3 minutes, with continuous mixing maintained after each addition. According to [46], nanoparticles, such as NA and NL, were initially dispersed in a portion of water and alkaline solution using a hand-electric mixer. The dispersed nanoparticles were then incorporated into the main mixture. To ensure homogeneity, the fresh concrete was hand-mixed for an additional 2–3 minutes before being evaluated for its fresh properties and subsequently cast. The GPC mixture was poured into molds of cubes, cylinders, and prisms until completely filled, and following casting, the specimens were covered

Table 5. The mixing proportions of ternary and Quaternary mixes

Mix No.	Mix Grade	L/B	Quantities of ingredients (kg/m³)									
			Binder	FA (%)	MK (%)	NA (%)	NL (%)	NaOH	Na_2SiO_3	Fine Agg.	Coarse Agg.	SP %
M13	GP-40	0.52	415	0.7	0.3	2	0	72	144	748	1030	1.2
M14	GP-40	0.52	415	0.7	0.3	3	0	72	144	748	1030	1.2
M15	GP-40	0.52	415	0.7	0.3	4	0	72	144	748	1030	1.2
M16	GP-40	0.52	415	0.7	0.3	0	2	72	144	748	1030	1.2
M17	GP-40	0.52	415	0.7	0.3	0	3	72	144	748	1030	1.2
M18	GP-40	0.52	415	0.7	0.3	0	4	72	144	748	1030	1.2
M19	GP-40	0.52	415	0.7	0.3	2	3	72	144	720	947	1.2
M20	GP-60	0.47	520	0.7	0.3	2	0	81	162	720	947	1.5
M21	GP-60	0.47	520	0.7	0.3	3	0	81	162	720	947	1.5
M22	GP-60	0.47	520	0.7	0.3	4	0	81	162	720	947	1.5
M23	GP-60	0.47	520	0.7	0.3	0	2	81	162	720	947	1.5
M24	GP-60	0.47	520	0.7	0.3	0	3	81	162	720	947	1.5
M25	GP-60	0.47	520	0.7	0.3	0	4	81	162	720	947	1.5
M26	GP-60	0.47	520	0.7	0.3	2	3	81	162	720	947	1.5

with nylon sheets to prevent the evaporation of the alkaline solution [47] and left for 24 hours under ambient conditions before demolding, as shown in Figure 1.

The specimens were subjected to curing in a laboratory oven at 60 °C for 24 hours after demolding, followed by curing at room temperature (between 22 and 30 °C) with the specimens covered by plastic sheets until the day of testing. These conditions were chosen to accelerate the geopolymerization process and enhance the binder reaction effectively. The 60 °C temperature promotes faster reaction, while the plastic covers help maintain moisture and prevent moisture loss, ensuring continuous curing in a stable environment [48].

The molds used for specimen preparation included (50 × 50 × 50) mm cubes for mortar compressive strength to determine the pozzolanic activity of the materials, (100 × 100 × 100) mm cubes for compressive strength and UPV, (100 × 200) mm cylinders for splitting tensile strength, and (100 × 100 × 400) mm prisms for flexural strength.

The comprehensive capturing of the mechanical behavior of the hardened state of GPC has been done using the tests of bulk density, compressive strength, splitting tensile strength, flexural strength, and ultrasonic pulse velocity (UPV) tests which gives a holistic understanding of the structural behavior GPC compared to the conventional OPC concrete. Bulk density was obtained after 7 and 28 days as per ASTM [49] using three 100×100×100 mm cubes for each mix as a result of the fact that higher density is usually indicative of lesser voids and higher porosity, which in turn translates to strength, durability, and permeability of the concrete. Compressive strength is really the key property when it comes to understanding how geopolymerization is going. To measure it, we tested 100 mm cube samples at 3, 7, 28, 56, and 90 days, following BS EN [50]. We used a digital testing machine (1900 kN capacity, see Figure 2-A) and kept the loading rate steady at 0.3 MPa per second. For splitting tensile strength-which shows how brittle materials like concrete handle tension-we used 100×200 mm cylinders, testing them at 7, 28, and 90 days according to ASTM C496-08 [51], again with the same 1900 kN machine. Plywood strips were placed above and below the specimens to ensure uniform load distribution (Figure 2b). A reduced specimen size was adopted, compared to the standard 150 × 300 mm dimensions, to minimize the required quantities of geopolymer and nanomaterial components, facilitate casting and handling, and accommodate laboratory equipment limitations, while maintaining the same aspect ratio (L/D = 2.0) to ensure comparable stress distribution. Therefore, this factor was taken into account when interpreting the results and comparing them with previous studies that used standard-sized specimens [52]. Flexural tensile strength was measured on 100×100×400 mm concrete prisms using a digital testing machine with a capacity of 150 kN, following the third-point loading method in accordance with ASTM [53], and tests were conducted specifically at 28 days (Figure 2c), with the average results of three prisms recorded for each mix. In addition to destructive tests, non-destructive evaluation was conducted using the UPV test to assess internal homogeneity and detect potential microcracks without damaging the specimens, following ASTM [54]..

Figure 1. Prepared samples of casting samples

The test used the same 100 mm cube specimens prepared for compressive strength at 3, 7, 28, 56, and 90 days (Figure 3) and was carried out with a portable ultrasonic non-destructive digital indicating tester (PUNDIT) equipped with 54 kHz (±5 kHz) piezoelectric transducers, with a thin grease layer applied to ensure effective coupling between the transducers and the concrete surface.

RESULTS AND DISCUSSIONS

Strength activity index

The results of the strength activity index (SAI) for the different mixes at 7 and 28 days, as shown in Table 6, highlight the influence of various additives on the mechanical performance of geopolymer concrete.

Figure 2. Mechanical tests of geopolymer concrete: (a) compressive strength, (b) splitting tensile strength, (c) flexural strength

Figure 3. Ultrasonic pulse velocity test

Fly ash exhibited SAI values of 87% at 7 days and 98% at 28 days, indicating relatively low pozzolanic activity, likely due to its low calcium content, which slows early-age strength development. Metakaolin showed moderate improvement, with SAI values of 92% and 102%, attributed to its fine, amorphous structure that enhances pozzolanic reactions and matrix strength. Nano-alumina demonstrated a significant increase in SAI to 134% at 7 days and 152% at 28 days, reflecting its role in improving microstructural packing and matrix density. Similarly, nano-lime increased SAI to 129% and 143%, enhancing the alumina-silica reactions and overall mechanical properties. These results indicate that nanomaterials such as nano-alumina and nano-lime substantially improve the early-age strength and reduce porosity in geopolymer concrete, while metakaolin provides moderate enhancement, and fly ash shows the least improvement due to slower pozzolanic activity. Therefore, the inclusion of nanomaterials is recommended to boost mechanical performance, particularly in applications requiring high early strength [35, 55, 56].

Slump test

The results presented in Figures 4 and 5 clearly demonstrate the overall trend in the workability of geopolymer concrete (GPC) mixtures. In the binary blends (FA–MK), increasing the proportion of metakaolin (MK) consistently led to a reduction in slump values. For example, the slump decreased from 165 mm in mix M1 (100% FA) to 121 mm in mix M6 (50% FA–50% MK) at a constant liquid-to-binder ratio (L/B) of 0.52. A similar pattern was observed at L/B = 0.47, where the slump value was 155 mm for M7 but dropped to 113 mm for M12.

Table 6. Strength activity index of fly ash, metakaolin and nanoparticles

Mixes	Strength Activity Index (SAI) (%), at 7 days	Strength Activity Index (SAI) (%), at 28 days
Control-PC	100	100
Fly ash	87	98
Metakaolin	92	102
Nano alumina	134	152
Nano lime	129	143

This reduction in workability can be attributed to the higher surface area and more reactive nature of MK particles compared to FA, which increase water demand and reduce fluidity. These findings are consistent with those reported by [57], who found that higher MK content in geopolymer mixtures decreases workability due to its high fineness and rapid dissolution rate.

In the ternary and quaternary blends (Figure 5), the inclusion of NA and NL further decreased the slump values compared to the binary blends. For instance, mix M13 (with 2% NA) achieved a slump of 130 mm, but when the NA content increased to 4% (M15), the slump decreased to 123 mm. A similar reduction was observed with NL replacement, where mix M16 (2% NL) recorded 116 mm, while M18 (4% NL) dropped to 109 mm.

The quaternary mixtures containing both NA and NL showed the greatest reduction in slump, with mix M26 recording only 100 mm at L/B = 0.47. The observed reduction in workability with the addition of NA and NL can be attributed to their ultrafine particle size and high surface area, which enhance nucleation and microstructural development but simultaneously increase water demand, resulting in lower flowability. These observations are consistent with previous studies [58, 59], which reported that the addition of nanoparticles tends to decrease workability due to particle agglomeration and the increased viscosity of the fresh mix.

Bulk density

The bulk density results (Table 7) exhibited a gradual increase with age, indicating successful geopolymerization and matrix densification. In binary mixes, the density increased from 2334–2348 kg/m³ at 7 days to 2347–2367 kg/m³ at 28 days, with a more pronounced rise observed in mixes with a lower L/B ratio (0.47) due to reduced water content and denser packing

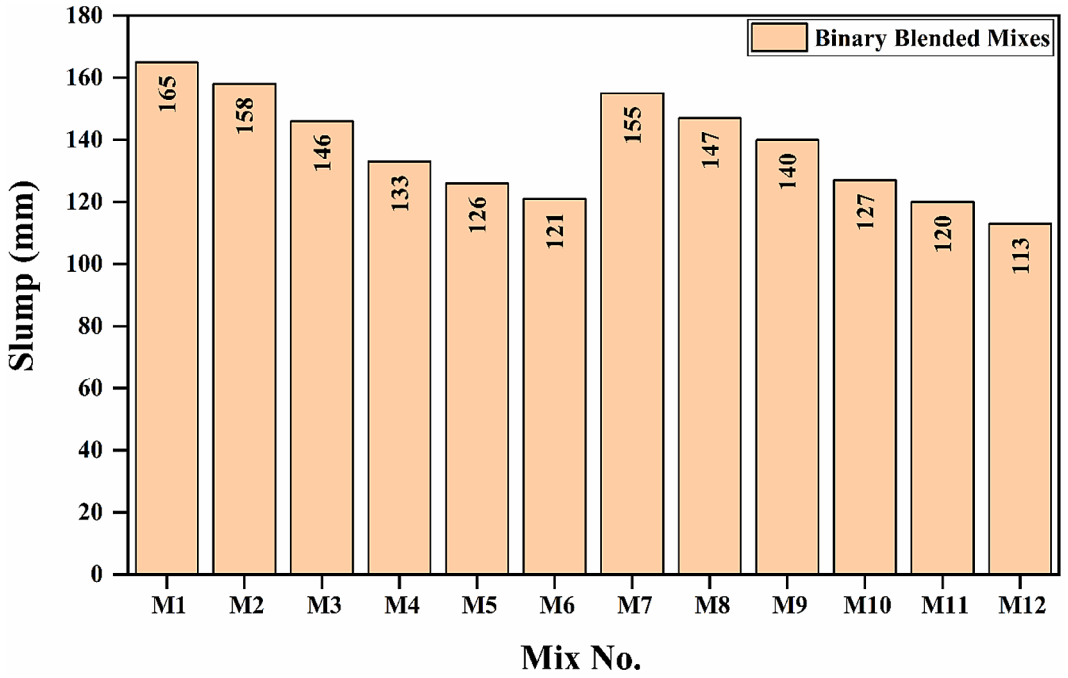

Figure 4. Slump results in binary blended mixes

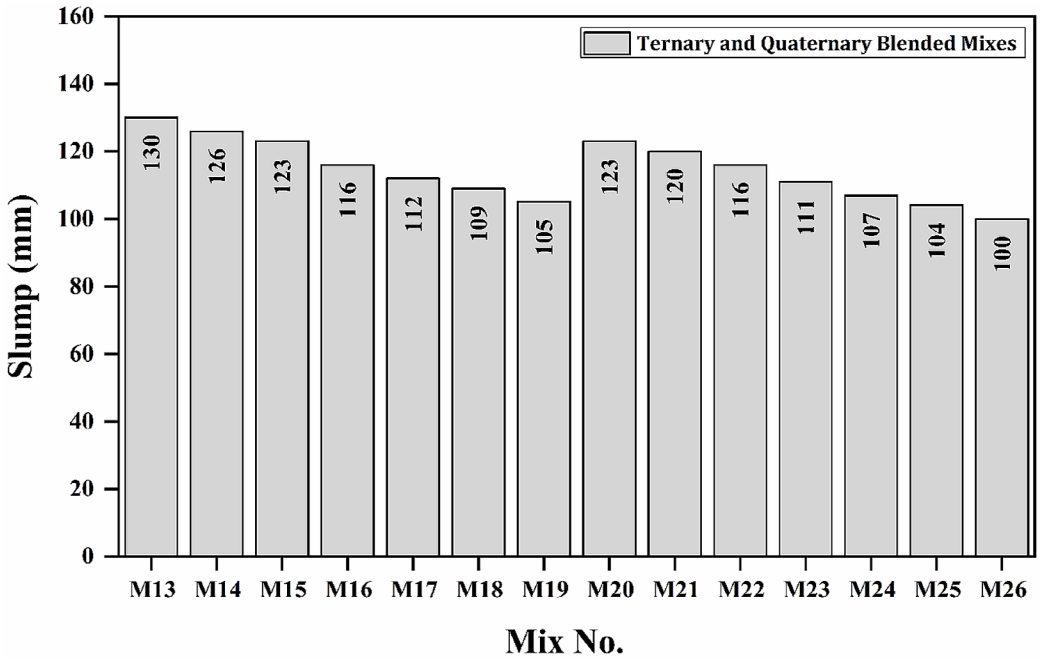

Figure 5. Slump results in ternary and quaternary blended mixes

Table 7. The results of bulk density tested of GPCs

Mix No.	Mix notation	Bulk density (kg/m³)	
		7days	28 days
M1	GP-100FA0MK-40	2334	2347
M2	GP-90FA10MK-40	2338	2349
M3	GP-80FA20MK-40	2341	2353
M4	GP-70FA30MK-40	2348	2367
M5	GP-60FA40MK-40	2347	2365
M6	GP-50FA50MK-40	2344	2361
M7	GP-100FA0MK-60	2343	2444
M8	GP-90FA10MK-60	2347	2447
M9	GP-80FA20MK-60	2349	2451
M10	GP-70FA30MK-60	2358	2458
M11	GP-60FA40MK-60	2354	2456
M12	GP-50FA50MK-60	2352	2453
M13	GP-70FA30MK-2NA0NL-40	2338	2389
M14	GP-70FA30MK-3NA0NL-40	2335	2386
M15	GP-70FA30MK-4NA0NL-40	2331	2379
M16	GP-70FA30MK-0NA2NL-40	2341	2393
M17	GP-70FA30MK-0NA3NL-40	2351	2397
M18	GP-70FA30MK-0NA4NL-40	2344	2391
M19	GP-70FA30MK-2NA3NL-40	2356	2406
M20	GP-70FA30MK-2NA0NL-60	2345	2478
M21	GP-70FA30MK-3NA0NL-60	2340	2470
M22	GP-70FA30MK-4NA0NL-60	2335	2471
M23	GP-70FA30MK-0NA2NL-60	2337	2472
M24	GP-70FA30MK-0NA3NL-60	2347	2481
M25	GP-70FA30MK-0NA4NL-60	2340	2467
M26	GP-70FA30MK-2NA3NL-60	2355	2489

of reaction products. In ternary and quaternary blends, the incorporation of nanoparticles NA and NL further enhanced the bulk density. For instance, mix M19 (2% NA + 3% NL) reached 2406 kg/m³ at 28 days, while mix M26 (2% NA + 3% NL at L/B = 0.47) achieved 2489 kg/m³, representing the highest value among all mixes. This improvement aligns with the findings of [60,61], which indicated that nanoparticles accelerate geopolymerization and refine the pore structure, leading to denser and stronger matrices.

These results highlight that controlling the addition of nanoparticles is critical for enhancing bulk density and achieving superior mechanical performance by producing a more compact and refined microstructure in geopolymer concrete.

Compressive strength

The compressive strength results of the binary mixes (FA–MK) presented in Figures (6, 7) demonstrate that incorporating metakaolin significantly enhanced strength development, particularly up to an optimum level of about 30% replacement. For the GP-40 series, strength increased gradually from 49.3 MPa at 90 days in the control mix M1 (100% FA) to 52.8 MPa in M4 (70% FA–30% MK). This improvement is mainly attributed to the high reactivity of metakaolin, which accelerates geopolymerization and promotes the formation of additional N-A-S-H and C-A-S-H gels, resulting in a denser matrix and reduced porosity. However, when MK content exceeded 30% (M5 and M6), the strength either stabilized or slightly declined (51.1–50.8 MPa at 90 days), due to the disruption in the Si/Al balance and the increased demand for alkalinity that could not be fully compensated, consistent with previous findings on FA–MK systems [62].

In contrast, the GP-60 series, which incorporated higher calcium content, exhibited a remarkable strength improvement starting from 28 days. The compressive strength increased sharply from 63.3 MPa in M7 to 66.3 MPa in M10 (30% MK), with further development reaching 71.4 MPa at 90 days. This behavior is attributed to the synergistic effect of slag, which provides reactive Ca^{2+} ions that facilitate the co-formation of C-(A)-S-H gel along with N-A-S-H gel, leading to a much denser microstructure and superior mechanical performance. The enhanced long-term strength of these mixes highlights the importance of balancing calcium-rich precursors with aluminosilicate-rich components to optimize binder gel formation [63].

Notably, the GP-40 and GP-60 series show different trends: while GP-40 exhibits a reduction in strength beyond 30% MK replacement, GP-60 continues to improve up to 50% MK. This difference can be attributed to variations in binder chemistry, gel formation, and interaction with the alkaline activator, which influence the geopolymerization kinetics and the resulting microstructure. Similar observations have been reported in other studies, where higher-calcium systems or higher activator reactivity enhanced gel formation and strength development even at higher MK contents [64]. The compressive strength results of the ternary and quaternary mixes presented in

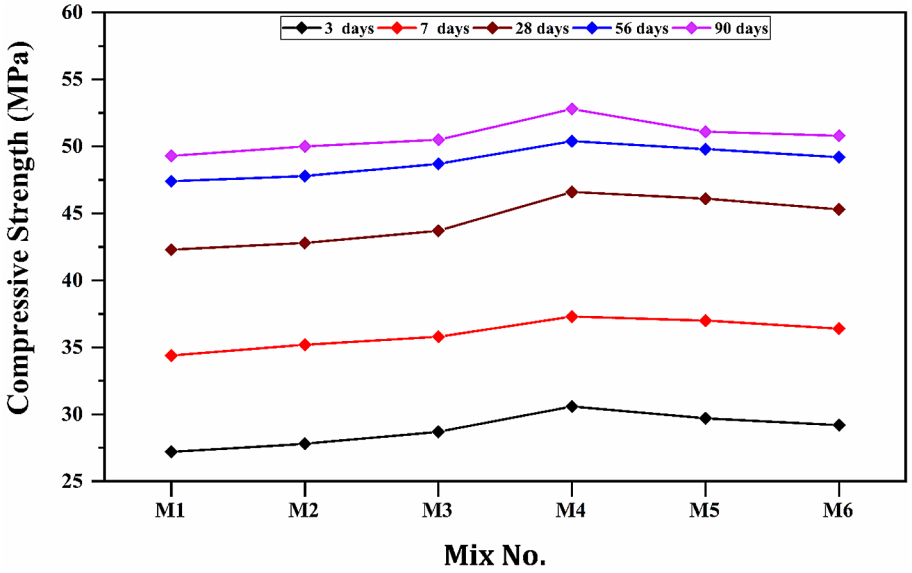

Figure 6. Compressive strength results of binary blended GP-40 mixes at different ages

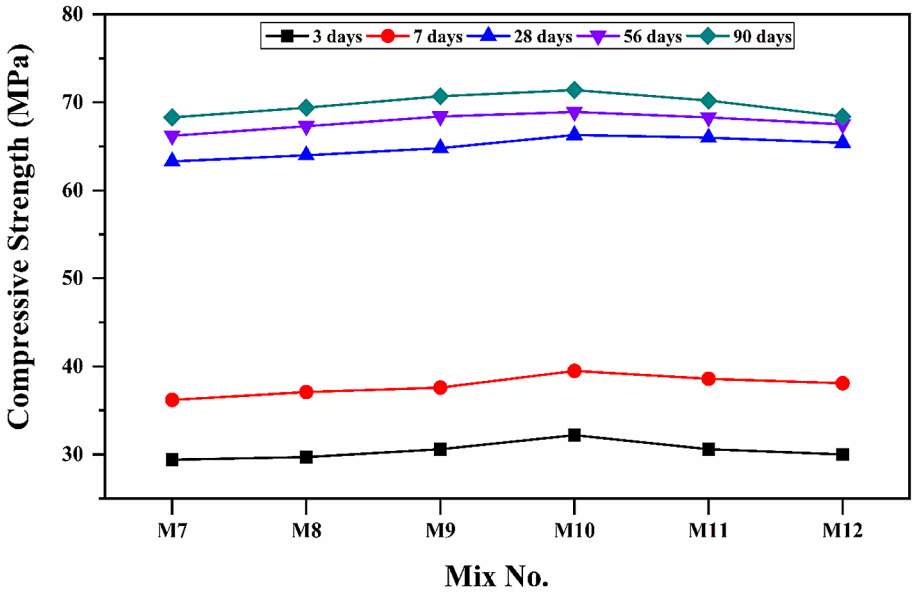

Figure 7. Compressive strength results of binary blended GP-60 mixes at different ages

Figures (8, 9) demonstrate the positive influence of incorporating nano-additives (NA and NL) into the FA–MK blends. For the GP-40 system, the results show that the addition of either Na_2O NA or NL improved the early- and later-age strengths compared to the binary blends. For example, mixes M13–M18 consistently outperformed the corresponding binary control (M4) at 28–90 days, achieving strengths in the range of 49–57 MPa, while M19 (containing both NA and NL) reached 58.7 MPa at 90 days, highlighting the synergistic effect of combining the two nanomaterials. This enhancement can be attributed to the nucleation effect of nanoparticles, which accelerates geopolymerization, promotes the formation of additional N-A-S-H and C-A-S-H gels, and refines the pore structure, leading to denser matrices.

For the GP-60 system, the strength development was even more remarkable. Ternary and quaternary mixes (M20–M26) showed substantial gains compared to the binary counterparts (M9–M12), with compressive strengths exceeding 70 MPa at 28 days and reaching up to 77.4 MPa in mix M26 at 90 days. The superior performance of these mixes is mainly attributed to the high reactivity of MK in a calcium-rich environment, combined with the nano-induced densification of the matrix. The presence of NA and NL particles not

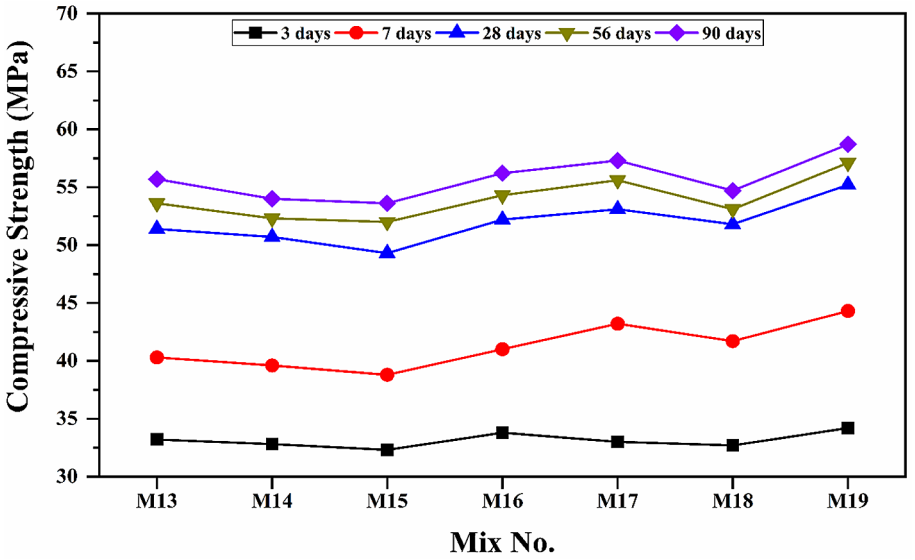

Figure 8. Compressive strength results of ternary and quaternary blended GP-40 mixes at different ages

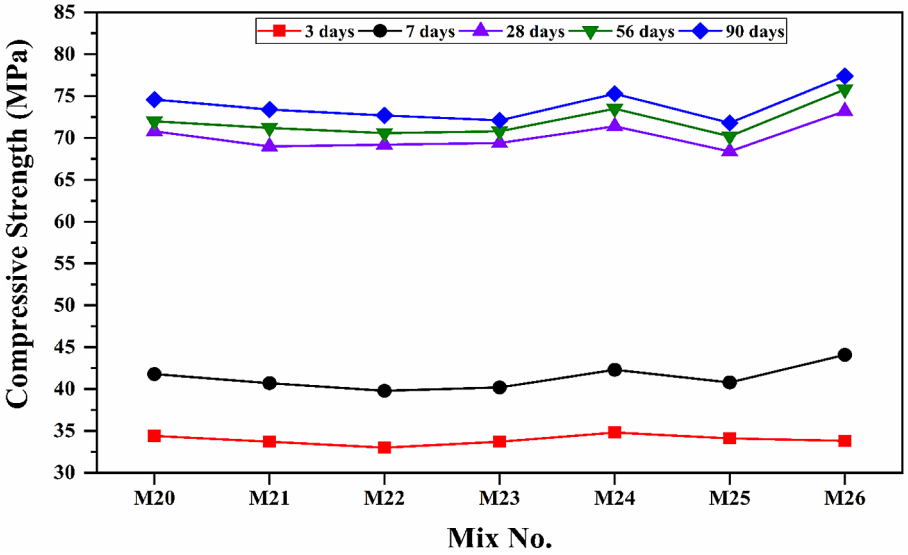

Figure 9. Compressive strength results of ternary and quaternary blended GP-60 mixes at different ages

only accelerated the dissolution of aluminosilicate precursors but also contributed to the refinement of the interfacial transition zone (ITZ), thereby improving the cohesion and load transfer capacity of the hardened paste. The observed improvements are consistent with published studies on nanomaterial incorporation in geopolymer systems, which report that nanoparticles act as nucleation centers and pore fillers, resulting in a compact microstructure with superior mechanical properties [65–67]. Furthermore, the continued strength gains up to 90 days aligns with previously reported geopolymer behavior, where these materials progressively develop strength due to the delayed hardening and evolution of the gel structure over time [64].

In general, the results can be summarized as follows: an optimal MK content (30%) enhances strength even in a low-calcium environment, while increasing slag/calcium content leads to rapid and significant improvements at all ages. Meanwhile, nanomaterials (NA and NL) play a crucial role in boosting strength and reducing porosity by enhancing microstructural packing and increasing the density of the geopolymer matrix.

Split tensile strength

The split tensile strength results of the binary geopolymer mixes presented in Figures (10, 11) reveal distinct trends governed by the proportion

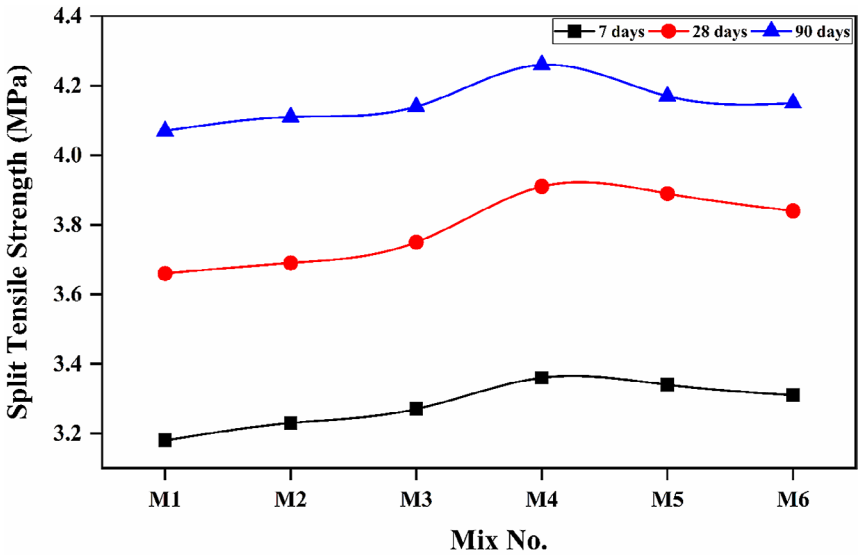

Figure 10. Split tensile strength results of binary blended GP-40 mixes at different ages

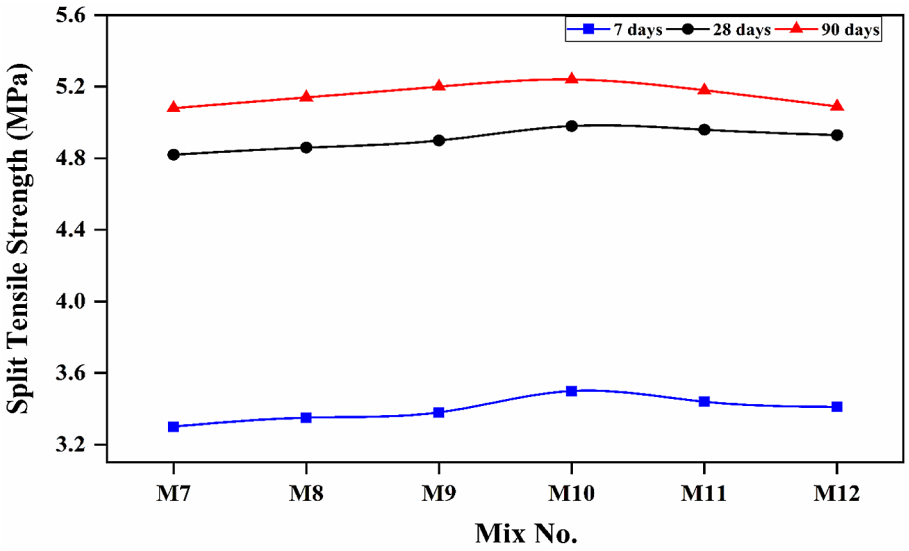

Figure 11. Split tensile strength results of binary blended GP-60 mixes at different ages

of FA and MK as well as the curing age. At 7 days, all mixes exhibited comparable tensile strength values ranging from 3.18–3.50 MPa, indicating that early-age performance is primarily influenced by the initial dissolution of reactive aluminosilicates rather than by mix composition. However, clear differences appeared at 28 and 90 days.

For the GP-40 system (M1–M6), increasing MK content from 0% to 30% significantly enhanced tensile strength, with mix M4 (GP-70FA30MK-40) reaching 3.91 MPa at 28 days compared to 3.66 MPa in the control mix (M1, GP-100FA0MK-40). At 90 days, the improvement trend continued, with M4 achieving 4.26 MPa, reflecting the beneficial role of MK in accelerating geopolymerization reactions and promoting the formation of additional N-A-S-H and C-A-S-H gels. However, beyond 30% MK replacement, the strength gains plateaued, as seen in mixes M5 and M6, where higher FA replacement limited reactivity due to the lower calcium content of FA. This behavior is in agreement with [68], which reported that excessive FA content results in slower geopolymerization kinetics, restricting tensile strength development.

For the GP-60 system (M7–M12), the impact of MK addition was more pronounced. Mix M10 (GP-70FA30MK-60) achieved the highest tensile strength, with 4.98 MPa at 28 days and 5.24 MPa at 90 days, representing a substantial improvement compared to M7 (GP-100FA0MK-60), which reached 4.82 MPa at 28 days and 5.08 MPa at 90 days. This enhancement can be attributed to the higher calcium content available in the GP-60 system, which facilitates faster geopolymerization and results in a denser microstructure with stronger interfacial bonding between binder particles and aggregates. Similar findings have been reported by [69], where increased calcium content in geopolymer systems significantly improved tensile strength and durability.

The split tensile strength results of the ternary and quaternary geopolymer mixes (Figures 12, 13) demonstrate a clear enhancement compared to the binary blends, particularly at 28 and 90 days. At early age (7 days), all mixes showed comparable values (3.45–3.78 MPa), but the influence of nanomaterials became evident with continued curing. The addition of nano-alumina (NA) and nano-limestone (NL) improved tensile strength by refining the pore structure, filling microvoids, and enhancing particle packing, which reduced porosity and promoted stronger interfacial bonding within the geopolymer matrix.

The GP-40 series (M13–M19) achieved moderate improvements, with the best performance recorded in the hybrid mix M19 (GP-70FA30MK-2NA3NL-40), which reached 4.58 MPa at 90 days. In contrast, the GP-60 series (M20–M26) showed significantly higher strengths, confirming the positive role of higher calcium availability in accelerating geopolymerization. Among these, M22 (GP-70FA30MK-4NA0NL-60) recorded the highest strength of 5.30 MPa at 90 days, while M26 (GP-70FA30MK-2NA3NL-60) also performed strongly with 5.53 MPa.

Overall, the results confirm that the combined effect of nanomaterials (NA and NL) and higher

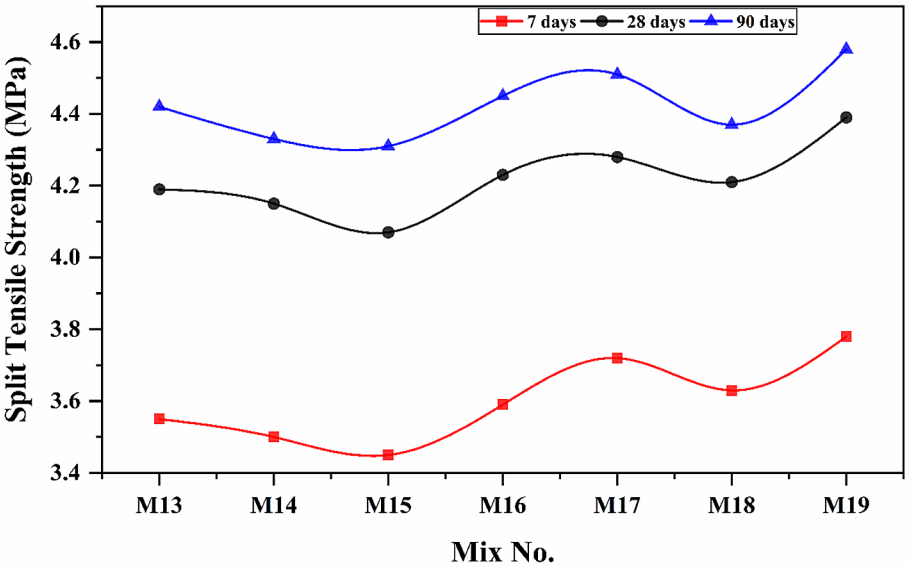

Figure 12. Split tensile strength results of ternary and quaternary blended GP-40 mixes at different ages

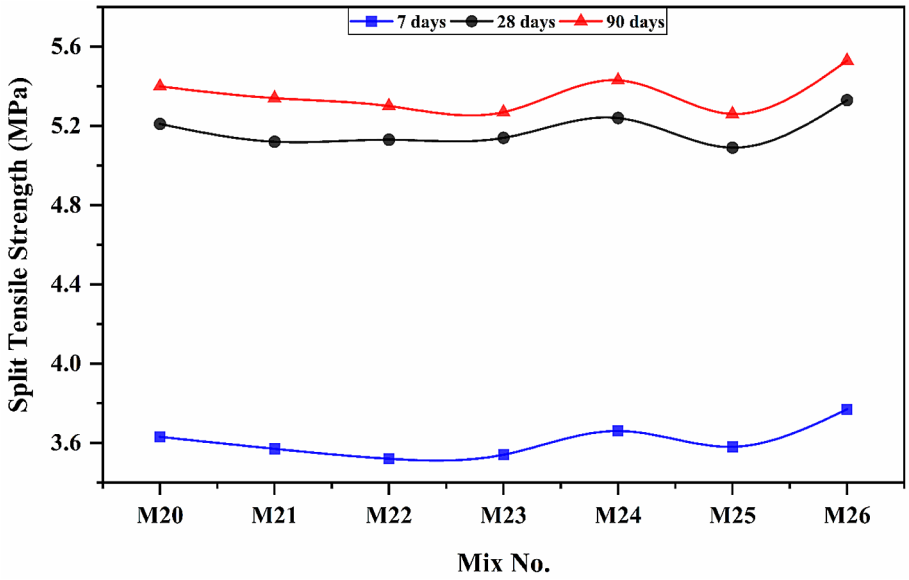

Figure 13. Split tensile strength results of ternary and quaternary blended GP-60 mixes at different ages

MK content (GP-60) provides a synergistic improvement in tensile strength. This enhancement is attributed to the densification of the matrix, improved gel formation, and better stress distribution, in agreement with findings reported by [70].

The highest tensile strength was observed when high MK content was combined with nanomaterials, indicating a synergistic effect that promotes denser microstructure, minimizes microcracks, and maximizes mechanical performance. Overall, increasing MK content gradually improves split tensile strength with age, low-calcium FA requires longer curing to reach full strength, and nanomaterials significantly enhance both tensile performance and microstructural density. The combination of high MK and nanomaterials produces the best results, confirming the synergistic interaction between mix components.

Flexural tensile strength

The flexural tensile strength results in Figures 14, 15 show a clear distinction between the two concrete grades: GP-40 and GP-60, and the effect of varying FA content on performance over time (7, 28, and 90 days).

For the GP-40 mixes, flexural strength values increased gradually with age, ranging from

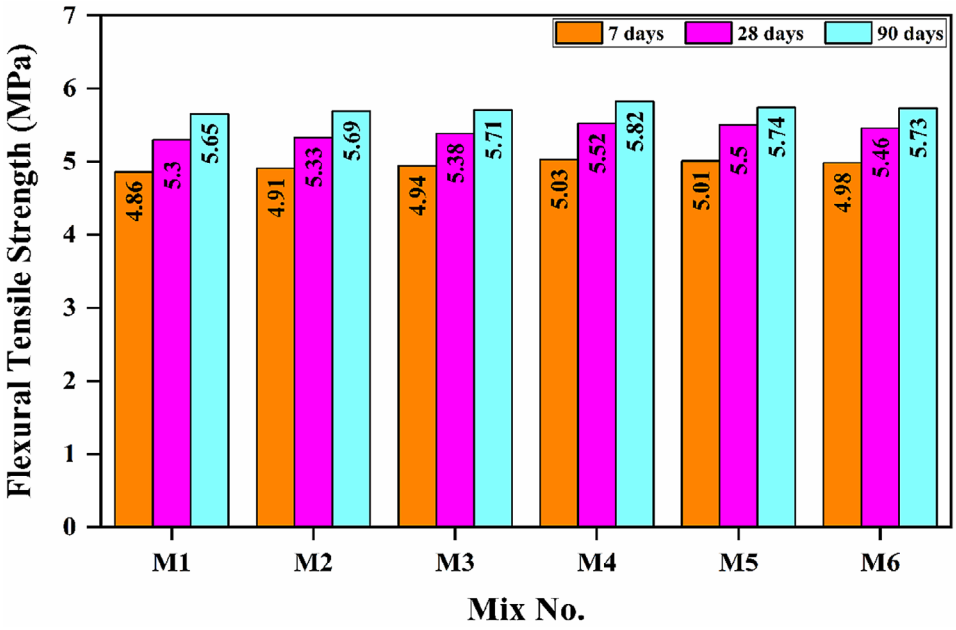

Figure 14. Flexural tensile strength results of binary blended GP-40 mixes at different ages

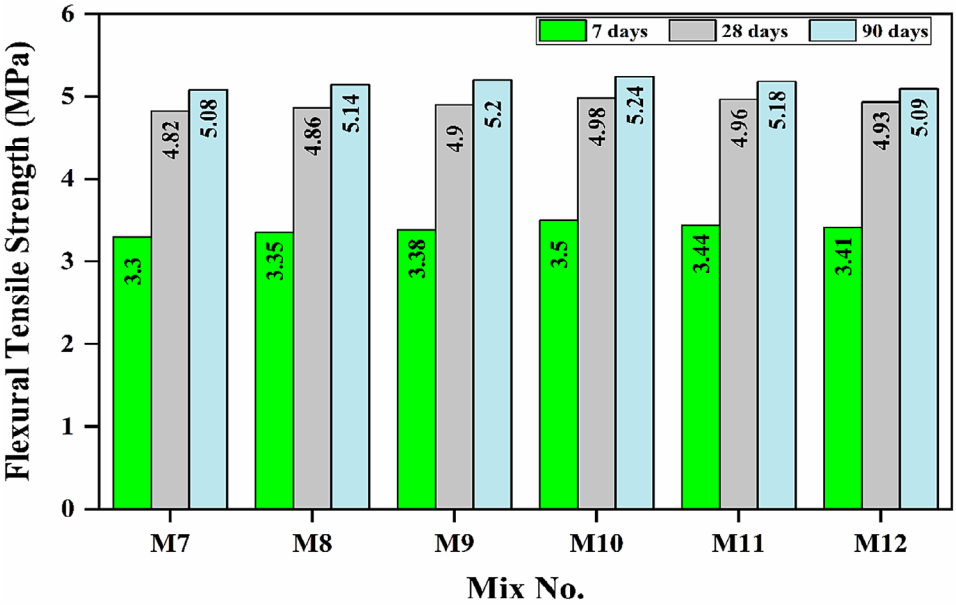

Figure 15. Flexural tensile strength results of binary blended GP-60 mixes at different ages

4.86–5.03 MPa at 7 days, 5.30–5.52 MPa at 28 days, and 5.65–5.82 MPa at 90 days. The highest strength within this grade was observed for M4 (GP-70FA30MK-40), indicating that a balanced FA/MK ratio optimizes the microstructure and gel formation, enhancing matrix cohesion. Slightly lower values at higher FA replacements (40–50%) suggest a minor reduction in strength due to lower reactivity of fly ash and a possible reduction in matrix density. In the GP-60 mixes, the flexural strength was significantly higher at all ages, ranging from 4.97–5.15 MPa at 7 days, 6.28–6.40 MPa at 28 days, and 6.48–6.61 MPa at 90 days, with M10 (GP-70FA30MK-60) achieving the peak value of 6.61 MPa at 90 days. The improvement in GP-60 compared to GP-40 can be attributed to the higher overall binder content and greater compressive strength grade, which enhances the formation of a denser and more cohesive geopolymer matrix, providing superior flexural performance. The results are consistent with previous findings reported in [71, 72], which confirmed that increasing MK content enhances both the mechanical performance and durability of geopolymer concrete. As shown

in Figures 16, 17, the inclusion of nanomaterials such as NA and NL further enhances flexural performance by acting as micro-fillers that reduce porosity and reinforce the interfacial transition zone (ITZ) between aggregates and the matrix, improving bonding and reducing cracking potential [67, 73, 74]. Additionally, the gradual increase in strength over time reflects the ongoing geopolymerization process, which continuously densifies the aluminosilicate network and improves structural integrity [75, 76]. Overall, ternary and quaternary blended mixes exhibit superior flexural performance compared to binary mixes due to the synergistic effects of MK and nanomaterial incorporation, which optimize microstructural packing and enhance mechanical properties [77].

Ultrasonic pulse velocity

The ultrasonic pulse velocity (UPV) results for the binary mixes (Figures 18 and 19) reveal a consistent increase in UPV values with age, from

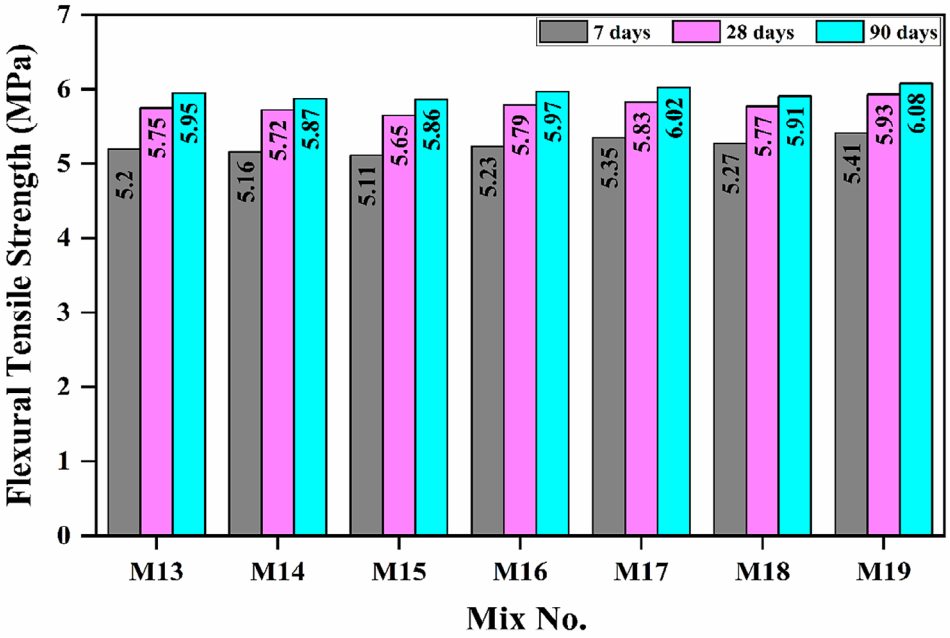

Figure 16. Flexural tensile strength results of ternary and quaternary blended GP-40 mixes at different ages

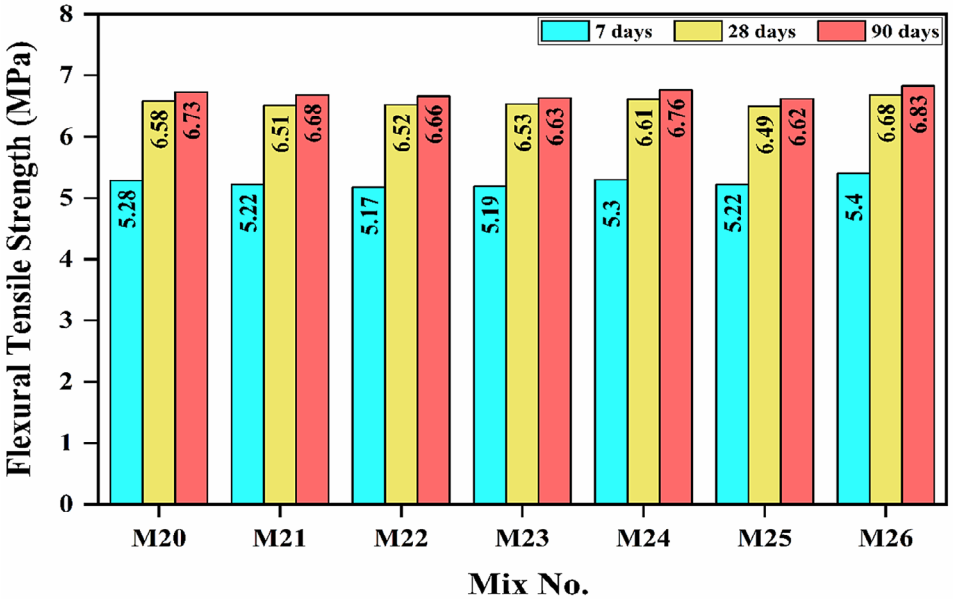

Figure 17. Flexural tensile strength results of ternary and quaternary blended GP-60 mixes at different ages

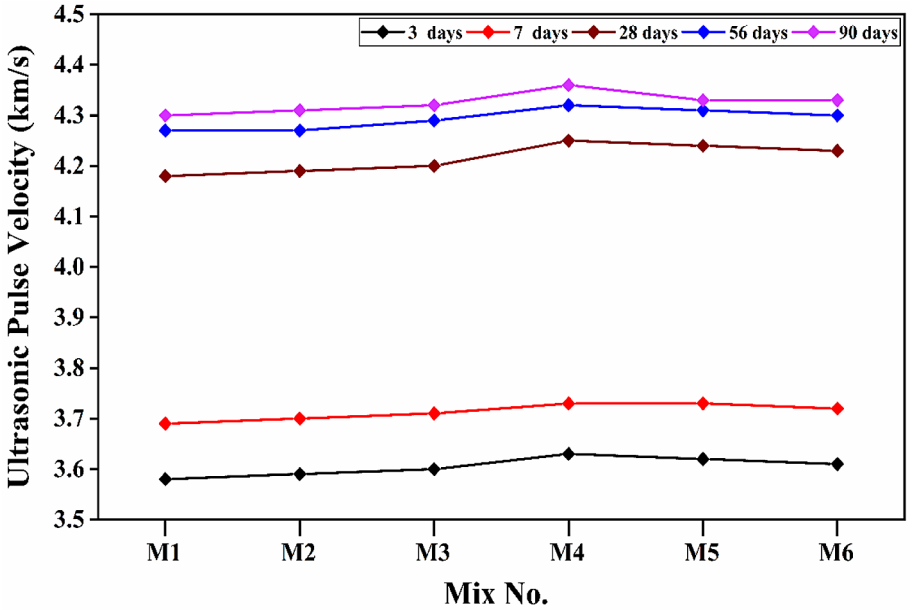

Figure 18. UPV results of binary blended GP-40 mixes at different ages

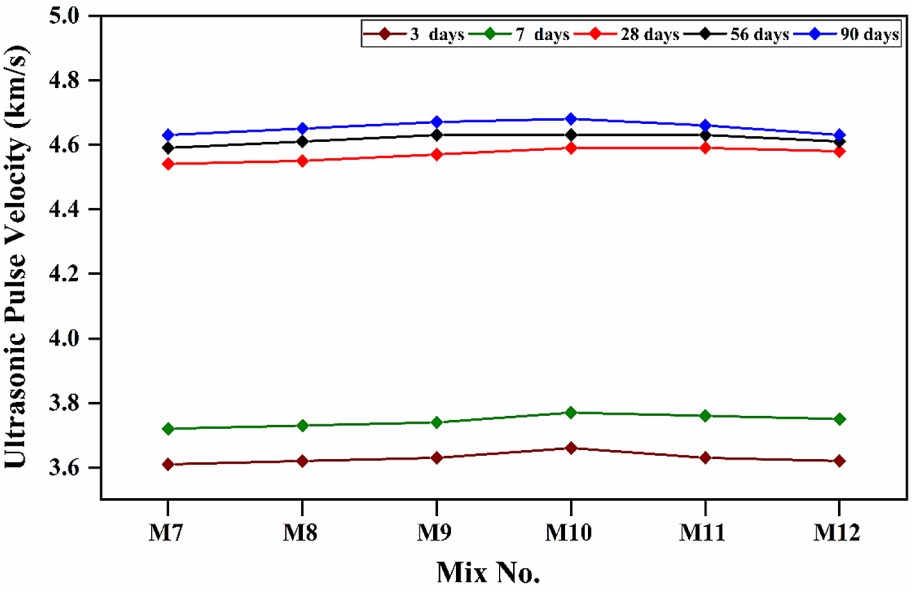

Figure 19. UPV results of binary blended GP-60 mixes at different ages

3 to 90 days. This continuous rise reflects the progressive geopolymerization reactions that enhance the internal cohesion of the matrix, leading to the formation of a denser and more compact microstructure over time [78, 79]. Regarding the influence of concrete strength grade, the GP-60 mixes consistently exhibited higher UPV values than the GP-40 mixes across all ages. For example, mix M3 (GP-40, FA 20%) achieved 4.32 km/s at 90 days, whereas M9 (GP-60, FA 20%) reached 4.67 km/s. This trend indicates that higher strength grades contribute to a more compact and cohesive matrix, improving particle bonding and minimizing internal voids. With respect to fly ash (FA) content, increasing FA from 0% to 50% in GP-40 mixes resulted in only marginal improvements in UPV at most ages. This can be attributed to the limited reactivity of FA compared to GGBS or MK, especially at early curing stages, although it contributes to the development of a finer geopolymeric gel. In contrast, FA interacted more effectively in the GP-60 mixes, producing relatively higher UPV values between 28 and 90 days. For instance, mix M10 (GP-60, FA 30%) attained 4.68 km/s at 90 days. This behavior demonstrates a synergistic effect between FA and higher

strength grades, improving matrix compactness and structural homogeneity.

Overall, all mixes showed continuous improvement in UPV values over time, indicating progressive matrix densification. The consistently higher values recorded for GP-60 mixes confirm that higher strength grades enhance internal integrity and durability. These observations align with previous studies [13], which reported that combining FA with highly reactive precursors such as GGBS or MK increases matrix density, strengthens the interfacial transition zone (ITZ), and refines the pore structure—resulting in improved UPV performance.

The results of the ternary and quaternary mixes (Figures 20 and 21) further support these findings. Mixes containing nano-additives (NA or NL) exhibited significantly higher UPV values than the binary ones, particularly at later ages (>28 days). Among these, the quaternary mixes incorporating both NA and NL (e.g., M19 and M26) achieved the highest UPV values, suggesting that nano-additives play a key role in improving microstructural packing, reducing fine porosity, and thereby enhancing ultrasonic conductivity.

This improvement is consistent with international research [80], which demonstrates that nano-additives act as ultra-fine fillers that increase

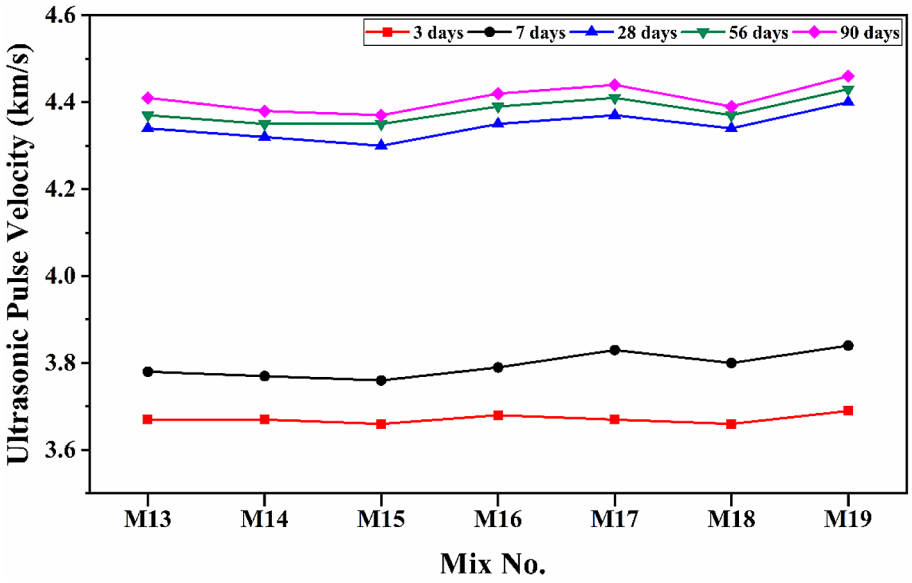

Figure 20. UPV results of ternary and quaternary blended GP-40 mixes at different ages

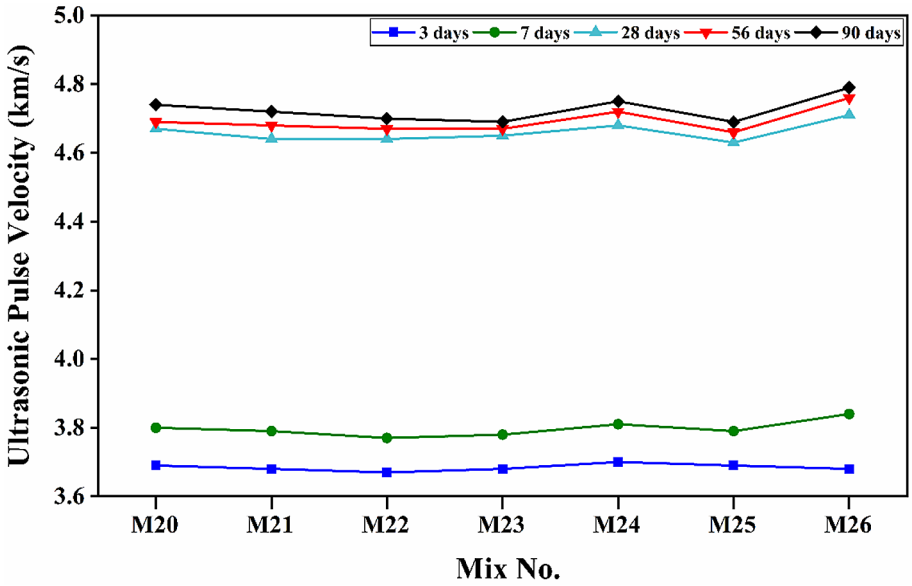

Figure 21. UPV results of ternary and quaternary blended GP-60 mixes at different ages

density and strengthen the ITZ between aggregates and the binder matrix. As the proportion of MK increased or nano-additives were introduced, the internal matrix density improved while overall porosity decreased, resulting in higher UPV values. The elevated UPV readings at 90 days confirm the ongoing enhancement of the geopolymer matrix over time, especially in the quaternary systems combining high MK, FA, and nano-additives (NA/NL).

CONCLUSIONS

The experimental investigation evaluated the mechanical performance of geopolymer concrete incorporating FA, MK, and nanomaterials, using compressive, tensile, flexural, and UPV tests to provide a comprehensive understanding of the effects of mix composition and curing age on material properties. The incorporation of NA and NL significantly improved both early- and later-age compressive strength by enhancing microstructural packing, reducing porosity, and promoting densification of the geopolymer matrix.

A metakaolin replacement level of 30% was identified as optimal for both low- and high-calcium systems, as it accelerated the geopolymerization process, promoted additional gel formation (N-A-S-H and C-(A)-S-H), and increased overall mechanical performance. Ternary and quaternary mixes combining MK with nanomaterials achieved the highest compressive strengths, reaching up to 77.4 MPa at 90 days, along with superior split tensile strength, demonstrating a synergistic effect that enhanced load-bearing capacity while reducing microcracks.

Flexural strength also showed notable improvement in mixes containing both MK and nanomaterials, reflecting better interfacial bonding, reduced cracking potential, and a denser, more homogeneous matrix structure. UPV measurements confirmed the progressive densification of the geopolymer matrix over time, with quaternary mixes exhibiting the highest values, highlighting the effectiveness of incorporating MK and nanomaterials in enhancing internal cohesion and overall performance of geopolymer concrete.

The locally sourced fly ash and metakaolin used in this study may differ in chemical composition, fineness, and reactivity from those employed in previous benchmark studies. As a result, the observed geopolymerization behavior and mechanical performance are specific to these materials and may not be directly applicable to other sources.

This study investigated only two nanomaterials, NA and NL. Other potentially effective nanomaterials, such as nano-silica or carbon-based additives, were not explored. Future studies are recommended to examine a broader range of nanomaterials to further enhance the performance of geopolymer concrete. The optimal mix (70% FA, 30% MK, 2% NA, 3% NL) was verified using materials from a single source. To generalize the findings, further testing with different material sources and varying dosages is required. This limitation has been acknowledged to highlight that the results may vary under different conditions.

The study did not include an economic or environmental assessment of the proposed mixes compared to conventional concrete, which should be addressed in future research. The materials have inherent limitations: fly ash develops early-age strength slowly, while metakaolin is more reactive but reduces workability and increases mix stiffness. The study did not provide detailed testing procedures for fresh properties such as workability, setting time, or heat of hydration. This omission represents a methodological limitation and should be considered when interpreting the overall performance of the geopolymer mixes.

REFERENCES

1. Habert G, De Lacaillerie JBD, Roussel N. An environmental evaluation of geopolymer based concrete production: reviewing current research trends. Journal of Cleaner Production 2011;19:1229–38. https://doi.org/10.1016/j.jclepro.2011.03.012
2. Andrew RM. Global CO_2 emissions from cement production, 1928–2017. Earth System Science Data 2018;10:2213–39. https://doi.org/10.5194/essd-10-2213-2018
3. Environment UN, Scrivener KL, John VM, Gartner EM. Eco-efficient cements: Potential economically viable solutions for a low-CO_2 cement-based materials industry. Cement and Concrete Research 2018;114:2–26. https://doi.org/10.1016/j.cemconres.2018.03.015
4. Cheruvu R, Kameswara Rao B. Enhanced concrete performance and sustainability with fly ash and ground granulated blast furnace slag – a comprehensive experimental study. Advances in Science and Technology Research Journal 2024;18:161–74. https://doi.org/10.12913/22998624/186192

5. Martínez A, Miller SA. Life cycle assessment and production cost of geopolymer concrete: A meta-analysis. Resources, Conservation and Recycling 2025;215:108018. https://doi.org/10.1016/j.resconrec.2024.108018
6. Bărbulescu A, Hosen K. Cement industry pollution and its impact on the environment and population health: a review. Toxics 2025;13. https://doi.org/10.3390/toxics13070587
7. Hammond GP, Jones CI. Embodied energy and carbon in construction materials. Proceedings of the Institution of Civil Engineers-Energy 2008;161:87–98. https://doi.org/10.1680/ener.2008.161.2.87
8. Lloyd NA, Rangan BV. Geopolymer concrete: A review of development and opportunities. 35th conference on our world in concrete & structures, Singapore, 2010;25–7.
9. Patil S, Joshi D, Mangla D, Savvidis I. Recent development in geopolymer concrete: a review. Materials Today: Proceedings 2023. https://doi.org/10.1016/j.matpr.2023.04.046
10. Liu Z, Cai CS, Liu F, Fan F. Feasibility study of loess stabilization with fly ash–based geopolymer. Journal of Materials in Civil Engineering 2016;28:4016003. https://doi.org/10.1061/(ASCE)MT.1943-5533.000149.
11. Fan F, Liu Z, Xu G, Peng H, Cai CS. Mechanical and thermal properties of fly ash based geopolymers. Construction and Building Materials 2018;160:66–81. https://doi.org/10.1016/j.conbuildmat.2017.11.023
12. Van Deventer JSJ, Provis JL, Duxson P. Technical and commercial progress in the adoption of geopolymer cement. Minerals Engineering 2012;29:89–104. https://doi.org/10.1016/j.mineng.2011.09.009
13. Provis JL, Palomo A, Shi C. Advances in understanding alkali-activated materials. Cement and Concrete Research 2015;78:110–25. https://doi.org/10.1016/j.cemconres.2015.04.013
14. Alahmari TS, Abdalla TA, Rihan MAM. Review of recent developments regarding the durability performance of eco-friendly geopolymer concrete. Buildings 2023;13:3033. https://doi.org/10.3390/buildings13123033
15. ASTM 618/C618-17. Standard specification for coal fly ash and raw or calcined natural pozzolan for use in concrete. American Society for Testing and Materials 2017.
16. Alterary SS, Marei NH. Fly ash properties, characterization, and applications: A review. Journal of King Saud University - Science 2021;33:101536. https://doi.org/10.1016/j.jksus.2021.101536
17. Bhatt A, Priyadarshini S, Mohanakrishnan AA, Abri A, Sattler M, Techapaphawit S. Physical, chemical, and geotechnical properties of coal fly ash: A global review. Case Studies in Construction Materials 2019;11:e00263. https://doi.org/10.1016/j.cscm.2019.e00263
18. Liu Z, Takasu K, Koyamada H, Suyama H. A study on engineering properties and environmental impact of sustainable concrete with fly ash or GGBS. Construction and Building Materials 2022;316:125776. https://doi.org/10.1016/j.conbuildmat.2021.125776
19. Shukla BK, Gupta A, Gowda S, Srivastav Y. Constructing a greener future: A comprehensive review on the sustainable use of fly ash in the construction industry and beyond. Materials Today: Proceedings 2023;93:257–64. https://doi.org/10.1016/j.matpr.2023.07.179
20. Islam MJ, Ahmed T, Salehin MR, Sakib MS, Shariar MS, Hossain M. Physical, mechanical, and durability properties of concrete with class F fly ash. MIST International Journal of Science and Technology 2023:27–41. https://doi.org/10.47981/j.mijst.11(02)2023.430(27-41)
21. Yang K-H, Jung Y-B, Cho M-S, Tae S-H. Effect of supplementary cementitious materials on reduction of CO2 emissions from concrete. Journal of Cleaner Production 2015;103:774–83. https://doi.org/10.1016/j.jclepro.2014.03.018
22. Pavithra P, Srinivasula Reddy M, Dinakar P, Hanumantha Rao B, Satpathy BK, Mohanty AN. A mix design procedure for geopolymer concrete with fly ash. Journal of Cleaner Production 2016;133:117–25. https://doi.org/10.1016/j.jclepro.2016.05.041
23. Hassan A, Arif M, Shariq M. Effect of curing condition on the mechanical properties of fly ash-based geopolymer concrete. SN Applied Sciences 2019;1:1694. https://doi.org/10.1007/s42452-019-1774-8
24. Özkılıç YO, Celik AI, Tunc U, Karalar M, Deifalla A, Alomayri T, et al. The use of crushed recycled glass for alkali activated fly ash based geopolymer concrete and prediction of its capacity. Journal of Materials Research and Technology 2023;24:8267–81. https://doi.org/10.1016/j.jmrt.2023.05.079
25. Ayeni O, Onwualu AP, Boakye E. Characterization and mechanical performance of metakaolin-based geopolymer for sustainable building applications. Construction and Building Materials 2021;272:121938. https://doi.org/10.1016/j.conbuildmat.2020.121938
26. Rashad AM. Metakaolin as cementitious material: History, scours, production and composition–A comprehensive overview. Construction and Building Materials 2013;41:303–18. https://doi.org/10.1016/j.conbuildmat.2012.12.001
27. Singh SB, Murugan M. Effect of metakaolin on the properties of pervious concrete. Construction and Building Materials 2022;346:128476. https://doi.org/10.1016/j.conbuildmat.2022.128476

28. Uzbaş B, Aydın AC. Analysis of fly ash concrete with scanning electron microscopy and X-ray diffraction. Advances in Science and Technology Research Journal 2019;13:100–10. https://doi.org/10.12913/22998624/114178
29. Nuaklong P, Sata V, Chindaprasirt P. Properties of metakaolin-high calcium fly ash geopolymer concrete containing recycled aggregate from crushed concrete specimens. Construction and Building Materials 2018;161:365–73. https://doi.org/10.1016/j.conbuildmat.2017.11.152
30. Kou S, Poon C, Agrela F. Comparisons of natural and recycled aggregate concretes prepared with the addition of different mineral admixtures. Cement and Concrete Composites 2011;33:788–95. https://doi.org/10.1016/j.cemconcomp.2011.05.009
31. Furlani E, Maschio S, Magnan M, Aneggi E, Andreatta F, Lekka M, et al. Synthesis and characterization of geopolymers containing blends of unprocessed steel slag and metakaolin: The role of slag particle size. Ceramics International 2018;44:5226–32. https://doi.org/10.1016/j.ceramint.2017.12.131
32. Albidah A, Alghannam M, Abbas H, Almusallam T, Al-Salloum Y. Characteristics of metakaolin-based geopolymer concrete for different mix design parameters. Journal of Materials Research and Technology 2021;10:84–98. https://doi.org/10.1016/j.jmrt.2020.11.104
33. Saboo N, Shivhare S, Kori KK, Chandrappa AK. Effect of fly ash and metakaolin on pervious concrete properties. Construction and Building Materials 2019;223:322–8. https://doi.org/10.1016/j.conbuildmat.2019.06.185
34. Kijjanon A, Sumranwanich T, Saengsoy W, Tangtermsirikul S. Chloride penetration resistance, electrical resistivity, and compressive strength of concrete with calcined kaolinite clay, fly ash, and limestone powder. Journal of Materials in Civil Engineering 2023;35:4022462. https://doi.org/10.1061/(ASCE)MT.1943-5533.0004643
35. Samuvel Raj R, Prince Arulraj G, Anand N, Kanagaraj B, Lubloy E, Naser MZ. Nanomaterials in geopolymer composites: A review. Developments in the Built Environment 2023;13:100114. https://doi.org/10.1016/j.dibe.2022.100114
36. Labaran YH, Atmaca N, Tan M, Atmaca K, Aram SA, Kaky AT. Nano-enhanced concrete: unveiling the impact of nano-silica on strength, durability, and cost efficiency. Discover Civil Engineering 2024;1:116. https://doi.org/10.1007/s44290-024-00120-9
37. Zhang P, Su J, Guo J, Hu S. Influence of carbon nanotube on properties of concrete: A review. Construction and Building Materials 2023;369:130388. https://doi.org/10.1016/j.conbuildmat.2023.130388
38. Raveendran N, K V. Synergistic effect of nano silica and metakaolin on mechanical and microstructural properties of concrete: An approach of response surface methodology. Case Studies in Construction Materials 2024;20:e03196. https://doi.org/10.1016/j.cscm.2024.e03196
39. Sujitha VS, Raja S, Rusho MA, Yishak S. Advances and developments in high strength geopolymer concrete for sustainable construction – A review. Case Studies in Construction Materials 2025;22:e04669. https://doi.org/https://doi.org/10.1016/j.cscm.2025.e04669
40. Khale D, Chaudhary R. Mechanism of geopolymerization and factors influencing its development: a review. Journal of Materials Science 2007;42:729–46. https://doi.org/10.1007/s10853-006-0401-4.
41. Nagaraja A, Boregowda U, Khatatneh K, Vangipuram R, Nuvvusetty R, Kiran VS. Similarity based feature transformation for network anomaly detection. IEEE Access 2020;8:39184–96. https://doi.org/10.1109/ACCESS.2020.2975716
42. Rangan BV, Hardjito D, Wallah SE, Sumajouw DM. Studies on fly ash-based geopolymer concrete. Proceedings of the world congress geopolymer, Saint Quentin, France, 2005;28:133–7.
43. Xu H, Van Deventer JSJ. The geopolymerisation of alumino-silicate minerals. International Journal of Mineral Processing 2000;59:247–66. https://doi.org/10.1016/S0301-7516(99)00074-5
44. ASTM C33/C33M-16. Standard specification for concrete aggregate. American Society for Testing and Materials 2016.
45. ASTM C494/C494-05. Standard specification for chemical admixtures for concrete. American Standard for Testing and Materials; West Conshohocken, Pennsylvania, USA 2005.
46. Shahrajabian F, Behfarnia K. The effects of nano particles on freeze and thaw resistance of alkali-activated slag concrete. Construction and Building Materials 2018;176:172–8. https://doi.org/10.1016/j.conbuildmat.2018.05.033
47. Albukhaty S, Al-Bayati L, Al-Karagoly H, Al-Musawi S. Preparation and characterization of titanium dioxide nanoparticles and in vitro investigation of their cytotoxicity and antibacterial activity against Staphylococcus aureus and Escherichia coli. Animal Biotechnology 2022;33:864–70. https://doi.org/10.1080/10495398.2020.1842751
48. Mo B, Zhu H, Cui X, He Y, Gong S. Effect of curing temperature on geopolymerization of metakaolin-based geopolymers. Applied Clay Science 2014;99:144–8. https://doi.org/10.1016/j.clay.2014.06.024
49. ASTM C29/C29M–07. Standard Test Method for Bulk Density ("Unit Weight") and Voids in Aggregate. American Society for Testing and Materials 2007:1–5.
50. BS EN 12390-3. Testing hardened concrete.

Compressive Strength of Test Specimens, BS EN 2021:12390–3.

51. ASTM C496-08. Standard Test Method for Splitting Tensile Strength of Cylindrical Concrete Specimens. American Society for Testing and Materials 2008.
52. Mohmmad SH, Shakor P, Muhammad JH, Hasan MF, Karakouzian M. Sustainable alternatives to cement: synthesizing metakaolin-based geopolymer concrete using nano-silica. Construction Materials 2023;3:276–86. https://doi.org/10.3390/constrmater3030018
53. ASTM C78-08. Standard test method for flexural strength of concrete (Using Simple Beam with Third-Point Loading). American Society for Testing and Materials 2008.
54. ASTM C597-02. Standard test method for pulse velocity through concrete. American Society for Testing and Materials 2002.
55. Zhang H, Li H, Guo H, Li Y, Wei L. Mechanical properties of alkali activated geopolymer cement mortar for non vibratory compacted trench backfilling. Scientific Reports 2025;15:12347. https://doi.org/10.1038/s41598-025-96291-1.
56. Paruthi S, Rahman I, Husain A, Khan AH, Manea-Saghin A-M, Sabi E. A comprehensive review of nano materials in geopolymer concrete: Impact on properties and performance. Developments in the Built Environment 2023;16:100287. https://doi.org/10.1016/j.dibe.2023.100287
57. Duxson P, Provis JL, Lukey GC, van Deventer JSJ. The role of inorganic polymer technology in the development of 'green concrete.' Cement and Concrete Research 2007;37:1590–7. https://doi.org/10.1016/j.cemconres.2007.08.018
58. Duxson P, Fernández-Jiménez A, Provis JL, Lukey GC, Palomo A, van Deventer JSJ. Geopolymer technology: the current state of the art. Journal of Materials Science 2007;42:2917–33. https://doi.org/10.1007/s10853-006-0637-z
59. Kotop MA, El-Feky MS, Alharbi YR, Abadel AA, Binyahya AS. Engineering properties of geopolymer concrete incorporating hybrid nano-materials. Ain Shams Engineering Journal 2021;12:3641–7. https://doi.org/10.1016/j.asej.2021.04.022
60. Rashad AM. Effect of nanoparticles on the properties of geopolymer materials. Magazine of Concrete Research 2019;71:1283–301. https://doi.org/10.1680/jmacr.18.00289
61. Ranjbar N, Kuenzel C. Influence of preheating of fly ash precursors to produce geopolymers. Journal of the American Ceramic Society 2017;100:3165–74. https://doi.org/10.1111/jace.14848
62. Jiang T, Liu Z, Tian X, Wu J, Wang L. Review on the impact of metakaolin-based geopolymer's reaction chemistry, nanostructure and factors on its properties. Construction and Building Materials 2024;412:134760. https://doi.org/10.1016/j.conbuildmat.2023.134760
63. Ma Z, Dan H, Tan J, Li M, Li S. Optimization design of MK-GGBS based geopolymer repairing mortar based on response surface methodology. Materials 2023;16:1889. https://doi.org/10.3390/ma16051889
64. Haruna S, Mohammed BS, Wahab MMA, Kankia MU, Amran M, Gora AM. Long-term strength development of fly ash-based one-part alkali-activated binders. Materials 2021;14:4160. https://doi.org/10.3390/ma14154160
65. Ma B, Luo Y, Zhou L, Shao Z, Liang R, Fu J, et al. The influence of calcium hydroxide on the performance of MK-based geopolymer. Construction and Building Materials 2022;329:127224. https://doi.org/10.1016/j.conbuildmat.2022.127224
66. Deb PS, Sarker PK, Barbhuiya S. Effects of nano-silica on the strength development of geopolymer cured at room temperature. Construction and Building Materials 2015;101:675–83. https://doi.org/10.1016/j.conbuildmat.2015.10.044
67. Rahmawati C, Aprilia S, Saidi T, Aulia TB, Hadi AE. The effects of nanosilica on mechanical properties and fracture toughness of geopolymer cement. Polymers 2021;13:2178. https://doi.org/10.3390/polym13132178
68. Divvala S, M. SR. Early strength properties of geopolymer concrete composites: An experimental study. Materials Today: Proceedings 2021;47:3770–7. https://doi.org/10.1016/j.matpr.2021.03.002
69. Luo Y, Zhang Q, Wang D, Yang L, Gao X, Liu Y, et al. Mechanical and microstructural properties of MK-FA-GGBFS-based self-compacting geopolymer concrete composites. Journal of Building Engineering 2023;77:107452. https://doi.org/10.1016/j.jobe.2023.107452
70. Ünal MT, Gökçe HS, Ayough P, Alnahhal AM, Şimşek O, Nehdi ML. Nanomaterial and fiber-reinforced sustainable geopolymers: A systematic critical review. Construction and Building Materials 2023;404:133325. https://doi.org/10.1016/j.conbuildmat.2023.133325
71. Davidovits J. Geopolymer chemistry and applications. Geopolymer Institute; 2008.
72. Oualit M, Irekti A. Mechanical performance of metakaolin-based geopolymer mortar blended with multi-walled carbon nanotubes. Ceramics International 2022;48:16188–95. https://doi.org/10.1016/j.ceramint.2022.02.166
73. Singh NB, Saxena SK, Kumar M. Effect of nanomaterials on the properties of geopolymer mortars and concrete. Materials Today: Proceedings 2018;5:9035–40. https://doi.org/10.1016/j.matpr.2017.10.018
74. Çevik A, Alzeebaree R, Humur G, Niş A, Gülşan ME. Effect of nano-silica on the chemical durability and mechanical performance of fly ash based

geopolymer concrete. Ceramics International 2018;44:12253–64. https://doi.org/10.1016/j.ceramint.2018.04.009

75. Rajan MS, AnuPriya A. Development and properties of low-calcium fly ash-based geo polymer concrete. International Journal of Innovative Research in Advanced Engineering 2024;11:465–9. https://doi.org/10.26562/ijirae.2024.v1105.04
76. Chiranjeevi K, Abraham M, Rath B, Praveenkumar TR. Enhancing the properties of geopolymer concrete using nano-silica and microstructure assessment: a sustainable approach. Scientific Reports 2023;13:17302. https://doi.org/10.1038/s41598-023-44491-y
77. Shilar FA, Ganachari S V, Patil VB, Khan TMY, Almakayeel NM, Alghamdi S. Review on the relationship between nano modifications of geopolymer concrete and their structural characteristics. Polymers 2022;14. https://doi.org/10.3390/polym14071421
78. Davidovits J. Geopolymer cement. A Review Geopolymer Institute, Technical Papers 2013;21:1–11.
79. Nath P, Sarker PK. Fracture properties of GGBFS-blended fly ash geopolymer concrete cured in ambient temperature. Materials and Structures 2017;50:32. https://doi.org/10.1617/s11527-016-0893-6
80. Wang Y, Liu H, Nie Z, Xue R, Zhu W, Sun X. Experimental investigation into the influence of calcium aluminate cement on the micro-and macro-mechanical properties of the interfacial transition zone in geopolymer concrete. Developments in the Built Environment 2025;21:100618. https://doi.org/10.1016/j.dibe.2025.100618